

Search for the decay $\bar{B}^0 \rightarrow \Lambda_c^+ \bar{p} p \bar{p}$

J. P. Lees,¹ V. Poireau,¹ V. Tisserand,¹ E. Grauges,² A. Palano,^{3a,3b} G. Eigen,⁴ B. Stugu,⁴ D. N. Brown,⁵ L. T. Kerth,⁵ Yu. G. Kolomensky,⁵ M. J. Lee,⁵ G. Lynch,⁵ H. Koch,⁶ T. Schroeder,⁶ C. Hearty,⁷ T. S. Mattison,⁷ J. A. McKenna,⁷ R. Y. So,⁷ A. Khan,⁸ V. E. Blinov,^{9a,9c} A. R. Buzykaev,^{9a} V. P. Druzhinin,^{9a,9b} V. B. Golubev,^{9a,9b} E. A. Kravchenko,^{9a,9b} A. P. Onuchin,^{9a,9c} S. I. Serednyakov,^{9a,9b} Yu. I. Skovpen,^{9a,9b} E. P. Solodov,^{9a,9b} K. Yu. Todyshev,^{9a,9b} A. N. Yushkov,^{9a} D. Kirkby,¹⁰ A. J. Lankford,¹⁰ M. Mandelkern,¹⁰ B. Dey,¹¹ J. W. Gary,¹¹ O. Long,¹¹ C. Campagnari,¹² M. Franco Sevilla,¹² T. M. Hong,¹² D. Kovalskyi,¹² J. D. Richman,¹² C. A. West,¹² A. M. Eisner,¹³ W. S. Lockman,¹³ B. A. Schumm,¹³ A. Seiden,¹³ D. S. Chao,¹⁴ C. H. Cheng,¹⁴ B. Echenard,¹⁴ K. T. Flood,¹⁴ D. G. Hitlin,¹⁴ P. Ongmongkolkul,¹⁴ F. C. Porter,¹⁴ R. Andreassen,¹⁵ Z. Huard,¹⁵ B. T. Meadows,¹⁵ B. G. Pushpawela,¹⁵ M. D. Sokoloff,¹⁵ L. Sun,¹⁵ P. C. Bloom,¹⁶ W. T. Ford,¹⁶ A. Gaz,¹⁶ U. Nauenberg,¹⁶ J. G. Smith,¹⁶ S. R. Wagner,¹⁶ R. Ayad,^{17,*} W. H. Toki,¹⁷ B. Spaan,¹⁸ R. Schwierz,¹⁹ D. Bernard,²⁰ M. Verderi,²⁰ S. Playfer,²¹ D. Bettoni,^{22a} C. Bozzi,^{22a} R. Calabrese,^{22a,22b} G. Cibinetto,^{22a,22b} E. Fioravanti,^{22a,22b} I. Garzia,^{22a,22b} E. Luppi,^{22a,22b} L. Piemontese,^{22a} V. Santoro,^{22a} R. Baldini-Ferroli,²³ A. Calcaterra,²³ R. de Sangro,²³ G. Finocchiaro,²³ S. Martellotti,²³ P. Patteri,²³ I. M. Peruzzi,^{23,†} M. Piccolo,²³ M. Rama,²³ A. Zallo,²³ R. Contri,^{24a,24b} E. Guido,^{24a,24b} M. Lo Vetere,^{24a,24b} M. R. Monge,^{24a,24b} S. Passaggio,^{24a} C. Patrignani,^{24a,24b} E. Robutti,^{24a} B. Bhuyan,²⁵ V. Prasad,²⁵ M. Morii,²⁶ A. Adametz,²⁷ U. Uwer,²⁷ H. M. Lacker,²⁸ P. D. Dauncey,²⁹ U. Mallik,³⁰ C. Chen,³¹ J. Cochran,³¹ W. T. Meyer,³¹ S. Prell,³¹ H. Ahmed,³² A. V. Gritsan,³³ N. Arnaud,³⁴ M. Davier,³⁴ D. Derkach,³⁴ G. Grosdidier,³⁴ F. Le Diberder,³⁴ A. M. Lutz,³⁴ B. Malaescu,^{34,‡} P. Roudeau,³⁴ A. Stocchi,³⁴ G. Wormser,³⁴ D. J. Lange,³⁵ D. M. Wright,³⁵ J. P. Coleman,³⁶ J. R. Fry,³⁶ E. Gabathuler,³⁶ D. E. Hutchcroft,³⁶ D. J. Payne,³⁶ C. Touramanis,³⁶ A. J. Bevan,³⁷ F. Di Lodovico,³⁷ R. Sacco,³⁷ G. Cowan,³⁸ J. Bougher,³⁹ D. N. Brown,³⁹ C. L. Davis,³⁹ A. G. Denig,⁴⁰ M. Fritsch,⁴⁰ W. Gradl,⁴⁰ K. Griessinger,⁴⁰ A. Hafner,⁴⁰ E. Prencipe,⁴⁰ K. R. Schubert,⁴⁰ R. J. Barlow,^{41,§} G. D. Lafferty,⁴¹ E. Behn,⁴² R. Cenci,⁴² B. Hamilton,⁴² A. Jawahery,⁴² D. A. Roberts,⁴² R. Cowan,⁴³ D. Dujmic,⁴³ G. Sciolla,⁴³ R. Cheaib,⁴⁴ P. M. Patel,^{44,¶} S. H. Robertson,⁴⁴ P. Biassoni,^{45a,45b} N. Neri,^{45a} F. Palombo,^{45a,45b} L. Cremaldi,⁴⁶ R. Godang,^{46,**} P. Sonnek,⁴⁶ D. J. Summers,⁴⁶ M. Simard,⁴⁷ P. Taras,⁴⁷ G. De Nardo,^{48a,48b} D. Monorchio,^{48a,48b} G. Onorato,^{48a,48b} C. Sciacca,^{48a,48b} M. Martinelli,⁴⁹ G. Raven,⁴⁹ C. P. Jessop,⁵⁰ J. M. LoSecco,⁵⁰ K. Honscheid,⁵¹ R. Kass,⁵¹ J. Brau,⁵² R. Frey,⁵² N. B. Sinev,⁵² D. Strom,⁵² E. Torrence,⁵² H. Ahmed,⁵² E. Feltresi,^{53a,53b} M. Margoni,^{53a,53b} M. Morandin,^{53a} M. Posocco,^{53a} M. Rotondo,^{53a} G. Simi,^{53a} F. Simonetto,^{53a,53b} R. Stroili,^{53a,53b} S. Akar,⁵⁴ E. Ben-Haim,⁵⁴ M. Bomben,⁵⁴ G. R. Bonneaud,⁵⁴ H. Briand,⁵⁴ G. Calderini,⁵⁴ J. Chauveau,⁵⁴ Ph. Leruste,⁵⁴ G. Marchiori,⁵⁴ J. Ocariz,⁵⁴ S. Sitt,⁵⁴ M. Biasini,^{55a,55b} E. Manoni,^{55a} S. Pacetti,^{55a,55b} A. Rossi,^{55a} C. Angelini,^{56a,56b} G. Batignani,^{56a,56b} S. Bettarini,^{56a,56b} M. Carpinelli,^{56a,56b,††} G. Casarosa,^{56a,56b} A. Cervelli,^{56a,56b} F. Forti,^{56a,56b} M. A. Giorgi,^{56a,56b} A. Lusiani,^{56a,56c} B. Oberhof,^{56a,56b} E. Paoloni,^{56a,56b} A. Perez,^{56a} G. Rizzo,^{56a,56b} J. J. Walsh,^{56a} D. Lopes Pegna,⁵⁷ J. Olsen,⁵⁷ A. J. S. Smith,⁵⁷ R. Faccini,^{58a,58b} F. Ferrarotto,^{58a} F. Ferroni,^{58a,58b} M. Gaspero,^{58a,58b} L. Li Gioi,^{58a} G. Piredda,^{58a} C. Büniger,⁵⁹ O. Grünberg,⁵⁹ T. Hartmann,⁵⁹ T. Leddig,⁵⁹ H. Schröder,^{59,‡‡} C. Voß,⁵⁹ R. Waldi,⁵⁹ T. Auye,⁶⁰ E. O. Olaiya,⁶⁰ F. F. Wilson,⁶⁰ S. Emery,⁶¹ G. Hamel de Monchenault,⁶¹ G. Vasseur,⁶¹ Ch. Yèche,⁶¹ F. Anulli,^{62,‡‡} D. Aston,⁶² D. J. Bard,⁶² J. F. Benitez,⁶² C. Cartaro,⁶² M. R. Convery,⁶² J. Dorfan,⁶² G. P. Dubois-Felsmann,⁶² W. Dunwoodie,⁶² M. Ebert,⁶² R. C. Field,⁶² B. G. Fulsom,⁶² A. M. Gabareen,⁶² M. T. Graham,⁶² C. Hast,⁶² W. R. Innes,⁶² P. Kim,⁶² M. L. Kocian,⁶² D. W. G. S. Leith,⁶² P. Lewis,⁶² D. Lindemann,⁶² B. Lindquist,⁶² S. Luitz,⁶² V. Luth,⁶² H. L. Lynch,⁶² D. B. MacFarlane,⁶² D. R. Muller,⁶² H. Neal,⁶² S. Nelson,⁶² M. Perl,⁶² T. Pulliam,⁶² B. N. Ratcliff,⁶² A. Roodman,⁶² A. A. Salnikov,⁶² R. H. Schindler,⁶² A. Snyder,⁶² D. Su,⁶² M. K. Sullivan,⁶² J. Va'vra,⁶² A. P. Wagner,⁶² W. F. Wang,⁶² W. J. Wisniewski,⁶² M. Wittgen,⁶² D. H. Wright,⁶² H. W. Wulsin,⁶² V. Ziegler,⁶² W. Park,⁶³ M. V. Purohit,⁶³ R. M. White,^{63,§§} J. R. Wilson,⁶³ A. Randle-Conde,⁶⁴ S. J. Sekula,⁶⁴ M. Bellis,⁶⁵ P. R. Burchat,⁶⁵ T. S. Miyashita,⁶⁵ E. M. T. Puccio,⁶⁵ M. S. Alam,⁶⁶ J. A. Ernst,⁶⁶ R. Gorodeisky,⁶⁷ N. Guttman,⁶⁷ D. R. Peimer,⁶⁷ A. Soffer,⁶⁷ S. M. Spanier,⁶⁸ J. L. Ritchie,⁶⁹ A. M. Ruland,⁶⁹ R. F. Schwitters,⁶⁹ B. C. Wray,⁶⁹ J. M. Izen,⁷⁰ X. C. Lou,⁷⁰ F. Bianchi,^{71a,71b} F. De Mori,^{71a,71b} A. Filippi,^{71a} D. Gamba,^{71a,71b} S. Zambito,^{71a,71b} L. Lancieri,^{72a,72b} L. Vitale,^{72a,72b} F. Martinez-Vidal,⁷³ A. Oyanguren,⁷³ P. Villanueva-Perez,⁷³ J. Albert,⁷⁴ Sw. Banerjee,⁷⁴ F. U. Bernlochner,⁷⁴ H. H. F. Choi,⁷⁴ G. J. King,⁷⁴ R. Kowalewski,⁷⁴ M. J. Lewczuk,⁷⁴ T. Lueck,⁷⁴ I. M. Nugent,⁷⁴ J. M. Roney,⁷⁴ R. J. Sobie,⁷⁴ N. Tasneem,⁷⁴ T. J. Gershon,⁷⁵ P. F. Harrison,⁷⁵ T. E. Latham,⁷⁵ H. R. Band,⁷⁶ S. Dasu,⁷⁶ Y. Pan,⁷⁶ R. Prepost,⁷⁶ and S. L. Wu⁷⁶

(The BABAR Collaboration)

¹Laboratoire d'Annecy-le-Vieux de Physique des Particules (LAPP), Université de Savoie, CNRS/IN2P3, F-74941 Annecy-Le-Vieux, France

²Facultat de Física, Departament ECM, Universitat de Barcelona, E-08028 Barcelona, Spain

^{3a}INFN Sezione di Bari, I-70126 Bari, Italy

^{3b}Università di Bari, I-70126 Bari, Italy

⁴Institute of Physics, University of Bergen, N-5007 Bergen, Norway

- ⁵Lawrence Berkeley National Laboratory and University of California, Berkeley, California 94720, USA
- ⁶Institut für Experimentalphysik 1, Ruhr Universität Bochum, D-44780 Bochum, Germany
- ⁷University of British Columbia, Vancouver, British Columbia V6T 1Z1, Canada
- ⁸Brunel University, Uxbridge, Middlesex UB8 3PH, United Kingdom
- ^{9a}Budker Institute of Nuclear Physics SB RAS, Novosibirsk 630090, Russia
- ^{9b}Novosibirsk State University, Novosibirsk 630090, Russia
- ^{9c}Novosibirsk State Technical University, Novosibirsk 630092, Russia
- ¹⁰University of California at Irvine, Irvine, California 92697, USA
- ¹¹University of California at Riverside, Riverside, California 92521, USA
- ¹²University of California at Santa Barbara, Santa Barbara, California 93106, USA
- ¹³Institute for Particle Physics, University of California at Santa Cruz, Santa Cruz, California 95064, USA
- ¹⁴California Institute of Technology, Pasadena, California 91125, USA
- ¹⁵University of Cincinnati, Cincinnati, Ohio 45221, USA
- ¹⁶University of Colorado, Boulder, Colorado 80309, USA
- ¹⁷Colorado State University, Fort Collins, Colorado 80523, USA
- ¹⁸Technische Universität Dortmund, Fakultät Physik, D-44221 Dortmund, Germany
- ¹⁹Technische Universität Dresden, Institut für Kern- und Teilchenphysik, D-01062 Dresden, Germany
- ²⁰Laboratoire Leprince-Ringuet, Ecole Polytechnique, CNRS/IN2P3, F-91128 Palaiseau, France
- ²¹University of Edinburgh, Edinburgh EH9 3JZ, United Kingdom
- ^{22a}INFN Sezione di Ferrara, I-44122 Ferrara, Italy
- ^{22b}Dipartimento di Fisica e Scienze della Terra, Università di Ferrara, I-44122 Ferrara, Italy
- ²³INFN Laboratori Nazionali di Frascati, I-00044 Frascati, Italy
- ^{24a}INFN Sezione di Genova, I-16146 Genova, Italy
- ^{24b}Dipartimento di Fisica, Università di Genova, I-16146 Genova, Italy
- ²⁵Indian Institute of Technology Guwahati, Guwahati, Assam 781 039, India
- ²⁶Harvard University, Cambridge, Massachusetts 02138, USA
- ²⁷Physikalisches Institut, Universität Heidelberg, D-69120 Heidelberg, Germany
- ²⁸Institut für Physik, Humboldt-Universität zu Berlin, D-12489 Berlin, Germany
- ²⁹Imperial College London, London SW7 2AZ, United Kingdom
- ³⁰University of Iowa, Iowa City, Iowa 52242, USA
- ³¹Iowa State University, Ames, Iowa 50011-3160, USA
- ³²Jazan University, Jazan 22822, Saudi Arabia
- ³³Johns Hopkins University, Baltimore, Maryland 21218, USA
- ³⁴Laboratoire de l'Accélérateur Linéaire, Centre Scientifique d'Orsay, IN2P3/CNRS et Université Paris-Sud 11, F-91898 Orsay Cedex, France
- ³⁵Lawrence Livermore National Laboratory, Livermore, California 94550, USA
- ³⁶University of Liverpool, Liverpool L69 7ZE, United Kingdom
- ³⁷Queen Mary, University of London, London E1 4NS, United Kingdom
- ³⁸University of London, Royal Holloway and Bedford New College, Egham, Surrey TW20 0EX, United Kingdom
- ³⁹University of Louisville, Louisville, Kentucky 40292, USA
- ⁴⁰Institut für Kernphysik, Johannes Gutenberg-Universität Mainz, D-55099 Mainz, Germany
- ⁴¹University of Manchester, Manchester M13 9PL, United Kingdom
- ⁴²University of Maryland, College Park, Maryland 20742, USA
- ⁴³Laboratory for Nuclear Science, Massachusetts Institute of Technology, Cambridge, Massachusetts 02139, USA
- ⁴⁴McGill University, Montréal, Québec H3A 2T8, Canada
- ^{45a}INFN Sezione di Milano, I-20133 Milano, Italy
- ^{45b}Dipartimento di Fisica, Università di Milano, I-20133 Milano, Italy
- ⁴⁶University of Mississippi, University, Mississippi 38677, USA
- ⁴⁷Physique des Particules, Université de Montréal, Montréal, Québec H3C 3J7, Canada
- ^{48a}INFN Sezione di Napoli, I-80126 Napoli, Italy
- ^{48b}Dipartimento di Scienze Fisiche, Università di Napoli Federico II, I-80126 Napoli, Italy
- ⁴⁹National Institute for Nuclear Physics and High Energy Physics, NIKHEF, NL-1009 DB Amsterdam, Netherlands
- ⁵⁰University of Notre Dame, Notre Dame, Indiana 46556, USA
- ⁵¹Ohio State University, Columbus, Ohio 43210, USA
- ⁵²University of Oregon, Eugene, Oregon 97403, USA
- ^{53a}INFN Sezione di Padova, I-35131 Padova, Italy
- ^{53b}Dipartimento di Fisica, Università di Padova, I-35131 Padova, Italy

- ⁵⁴*Laboratoire de Physique Nucléaire et de Hautes Energies, IN2P3/CNRS, Université Pierre et Marie Curie-Paris6, Université Denis Diderot-Paris7, F-75252 Paris, France*
- ^{55a}*INFN Sezione di Perugia, I-06123 Perugia, Italy*
- ^{55b}*Dipartimento di Fisica, Università di Perugia, I-06123 Perugia, Italy*
- ^{56a}*INFN Sezione di Pisa, I-56127 Pisa, Italy*
- ^{56b}*Dipartimento di Fisica, Università di Pisa, I-56127 Pisa, Italy*
- ^{56c}*Scuola Normale Superiore di Pisa, I-56127 Pisa, Italy*
- ⁵⁷*Princeton University, Princeton, New Jersey 08544, USA*
- ^{58a}*INFN Sezione di Roma, I-00185 Roma, Italy*
- ^{58b}*Dipartimento di Fisica, Università di Roma La Sapienza, I-00185 Roma, Italy*
- ⁵⁹*Universität Rostock, D-18051 Rostock, Germany*
- ⁶⁰*Rutherford Appleton Laboratory, Chilton, Didcot, Oxon OX11 0QX, United Kingdom*
- ⁶¹*Centre de Saclay, CEA, Irfu, SPP, F-91191 Gif-sur-Yvette, France*
- ⁶²*SLAC National Accelerator Laboratory, Stanford, California 94309, USA*
- ⁶³*University of South Carolina, Columbia, South Carolina 29208, USA*
- ⁶⁴*Southern Methodist University, Dallas, Texas 75275, USA*
- ⁶⁵*Stanford University, Stanford, California 94305-4060, USA*
- ⁶⁶*State University of New York, Albany, New York 12222, USA*
- ⁶⁷*School of Physics and Astronomy, Tel Aviv University, Tel Aviv 69978, Israel*
- ⁶⁸*University of Tennessee, Knoxville, Tennessee 37996, USA*
- ⁶⁹*University of Texas at Austin, Austin, Texas 78712, USA*
- ⁷⁰*University of Texas at Dallas, Richardson, Texas 75083, USA*
- ^{71a}*INFN Sezione di Torino, I-10125 Torino, Italy*
- ^{71b}*Dipartimento di Fisica, Università di Torino, I-10125 Torino, Italy*
- ^{72a}*INFN Sezione di Trieste, I-34127 Trieste, Italy*
- ^{72b}*Dipartimento di Fisica, Università di Trieste, I-34127 Trieste, Italy*
- ⁷³*IFIC, Universitat de Valencia-CSIC, E-46071 Valencia, Spain*
- ⁷⁴*University of Victoria, Victoria, British Columbia V8W 3P6, Canada*
- ⁷⁵*Department of Physics, University of Warwick, Coventry CV4 7AL, United Kingdom*
- ⁷⁶*University of Wisconsin, Madison, Wisconsin 53706, USA*

(Received 6 January 2014; published 30 April 2014)

We report a search for the decay $\bar{B}^0 \rightarrow \Lambda_c^+ \bar{p} p \bar{p}$. Using a data sample of 471×10^6 $B\bar{B}$ pairs collected with the *BABAR* detector at the PEP-II2 storage ring at SLAC, we find no events and set an upper limit on the branching fraction $\mathcal{B}(\bar{B}^0 \rightarrow \Lambda_c^+ \bar{p} p \bar{p}) \times \frac{\mathcal{B}(\Lambda_c^+ \rightarrow p K^- \pi^+)}{0.050} < 2.8 \times 10^{-6}$ at 90% C.L., where we have normalized $\mathcal{B}(\Lambda_c^+ \rightarrow p K^- \pi^+)$ to the world average value.

DOI: 10.1103/PhysRevD.89.071102

PACS numbers: 13.25.Hw, 13.60.Rj, 14.20.Lq

B mesons have approximately 7% [1] baryons among their decay products. This is a substantial fraction justifying further investigations that may allow better understanding of baryon production in B decays and, more generally,

quark fragmentation into baryons. The measurement of exclusive branching fractions of baryonic B decays as well as systematic studies of the dynamics of the decay, i.e., the fraction of resonant subchannels, is a direct way for studying the mechanisms of hadronization into baryons.

We report herein a search for the decay $\bar{B}^0 \rightarrow \Lambda_c^+ \bar{p} p \bar{p}$ [2] using a dataset of about 424 fb^{-1} [3], corresponding to 471×10^6 $B\bar{B}$ pairs. This decay is closely related to $\bar{B}^0 \rightarrow \Lambda_c^+ \bar{p} \pi^+ \pi^-$ and $B^- \rightarrow \Lambda_c^+ \bar{p} \pi^+ \pi^- \pi^-$, which have a similar quark content and the (so far) largest measured branching fractions among the baryonic B decays with a Λ_c^+ in the final state. The CLEO Collaboration has measured the branching fraction $\mathcal{B}(B^- \rightarrow \Lambda_c^+ \bar{p} \pi^+ \pi^- \pi^-) = (23 \pm 7) \times 10^{-4}$ [4]. *BABAR* reported a measurement of $\mathcal{B}(\bar{B}^0 \rightarrow \Lambda_c^+ \bar{p} \pi^+ \pi^-) = (12.3 \pm 3.3) \times 10^{-4}$ as well as the branching ratios of resonant subchannels with $\Sigma_c(2455, 2520)^{0,++} \rightarrow \Lambda_c^+ \pi^- \pi^+$ [5]. The main differences between the decay presented here and the other two decay

*Present address: University of Tabuk, Tabuk 71491, Saudi Arabia.

†Also at Dipartimento di Fisica, Università di Perugia, Perugia, Italy.

‡Present address: Laboratoire de Physique Nucléaire et de Hautes Energies, IN2P3/CNRS, Paris, France.

§Present address: University of Huddersfield, Huddersfield HD1 3DH, United Kingdom.

¶Deceased.

**Present address: University of South Alabama, Mobile, Alabama 36688, USA.

††Also at Università di Sassari, Sassari, Italy.

‡‡Also at INFN Sezione di Roma, Roma, Italy.

§§Present address: Universidad Técnica Federico Santa María, Valparaíso 2390123, Chile.

channels are the absence of possible resonant subchannels and the much smaller phase space (PS), e.g.,

$$\frac{\int d\text{PS}(\bar{B}^0 \rightarrow \Lambda_c^+ \bar{p} p \bar{p})}{\int d\text{PS}(\bar{B}^0 \rightarrow \Lambda_c^+ \bar{p} \pi^+ \pi^-)} \approx \frac{1}{1500}. \quad (1)$$

Given the fact that the decay products of $\bar{B}^0 \rightarrow \Lambda_c^+ \bar{p} p \bar{p}$ are limited to a small PS, a significant deviation from the phase space factor of 1/1500 in the ratio of the branching fractions may occur if hadronization into $\Lambda_c^+ \bar{p}$ and/or $p \bar{p}$ is enhanced due to their generally low invariant masses. This phenomenon is known as threshold enhancement and describes the dynamically enhanced decay rate at the baryon-antibaryon-mass threshold. It has been observed in baryonic B decays with open charm final states [5–8], charmless baryonic B decays [9] and in the decay $J/\psi \rightarrow \gamma p \bar{p}$ [10]. An example where the decay with the smaller PS is preferred is the ratio of $\mathcal{B}(B^- \rightarrow \Lambda_c^+ \bar{\Lambda}_c^- K^-)/\mathcal{B}(B^- \rightarrow \Lambda_c^+ \bar{p} \pi^-) \approx 3$ [1] with $\int d\text{PS}(B^- \rightarrow \Lambda_c^+ \bar{\Lambda}_c^- K^-)/\int d\text{PS}(B^- \rightarrow \Lambda_c^+ \bar{p} \pi^-) \approx 1/70$. The influence of the weak interaction is expected to be similar here since $|V_{cs}| \approx |V_{ud}|$. General phenomenological approaches to describe the threshold enhancement consider, for example, gluonic and fragmentation mechanisms [11] and pole models [12]. In particular, an enhancement at the proton-antiproton mass threshold could be explained by the baryonium candidate $X(1835)$ [1,13,14]. Other theorists propose the possibility of S wave $p \bar{p}$ final state interaction with isospin $I = 1$ [15] and contributions from one-pion-exchange interactions in $N\bar{N}$ states with isospin $I = 1$ and spin $S = 0$ [16].

On the other hand, the decay $\bar{B}^0 \rightarrow \Lambda_c^+ \bar{p} p \bar{p}$ may be suppressed by the absence of resonant subchannels, which may play an important role for baryonic B decays, e.g., the resonant part of $\bar{B}^0 \rightarrow \Lambda_c^+ \bar{p} \pi^+ \pi^-$ due to Σ_c baryons is $\approx 40\%$ [5]. The size of the branching fraction may allow us to balance the relevance of resonant subchannels against PS in baryonic B decays.

This analysis is based on a data set that was collected with the *BABAR* detector at the PEP-II2 asymmetric-energy e^+e^- storage ring, which was operated at a center-of-mass (CM) energy equal to the $\Upsilon(4S)$ mass. We use EvtGen [17] and JETSET 7.4 74 [18] for simulation of *BABAR* events, and GEANT4 [19] for detector simulation. The sample of simulated decays $\bar{B}^0 \rightarrow \Lambda_c^+ \bar{p} p \bar{p}$ with $\Lambda_c^+ \rightarrow p K^- \pi^+$, both uniformly distributed in PS, is referred to as signal Monte Carlo (MC).

For the reconstruction of charged-particle tracks, the *BABAR* detector uses a tracking system that consists of a five-layer double-sided silicon vertex tracker surrounding the beam pipe followed by a 40-layer multiwire drift chamber with stereoangle configuration. A superconducting solenoid generates an approximately uniform magnetic field of 1.5 Tesla inside the tracking system which allows a precise measurement of the momentum of the tracks. The

selection of proton, kaon and pion candidates is based on measurements of the energy loss in the silicon vertex tracker and the drift chamber, and measurements of the Cerenkov radiation in the detector of internally reflected Cerenkov light [20]. A detailed description of the *BABAR* detector can be found elsewhere [21,22].

We reconstruct Λ_c^+ in the subchannel $\Lambda_c^+ \rightarrow p K^- \pi^+$. For the reconstruction of the B candidate, we fit the entire $\bar{B}^0 \rightarrow \Lambda_c^+ \bar{p} p \bar{p}$ decay tree simultaneously, including geometric constraints to the \bar{B}^0 and Λ_c^+ decay vertices, and require the χ^2 fit probability to exceed 0.1%.

Averaging over the momentum and polar angle of the particles that we use for our reconstruction in the signal MC sample, the track finding efficiency is larger than 97% [23]. The identification efficiency for protons and pions is about 99% and for kaons about 95% while the probability of a pion, kaon or proton to be misidentified is below 2%. In particular, the probability for a pion or kaon to be misidentified as a proton is negligible. Thus, we expect a low combinatoric background level due to the fact that three genuine protons originating from a common B vertex, like for $\bar{B}^0 \rightarrow \Lambda_c^+ \bar{p} p \bar{p}$, are rare in *BABAR* events.

To suppress background, we develop selection criteria for the $\bar{B}^0 \rightarrow \Lambda_c^+ \bar{p} p \bar{p}$ and $\Lambda_c^+ \rightarrow p K^- \pi^+$ candidates using correctly reconstructed decays in the signal MC sample.

For $p K^- \pi^+$ combinations from Λ_c^+ decays, we observe a narrow and a broad signal component in the $m_{pK\pi}$ invariant-mass distribution, in which the broad component results from badly reconstructed candidates. Thus, we fit the $m_{pK\pi}$ invariant-mass distribution to a sum of two Gaussian functions with a common mean value (Fig. 1). We extract a standard deviation (σ) of (3.74 ± 0.04) MeV/ c^2 for the narrow component and (15.4 ± 0.4) MeV/ c^2 for the broad component. The uncertainty is purely statistical. The fraction of the narrow part is approximately 80%. The mean value (μ) of

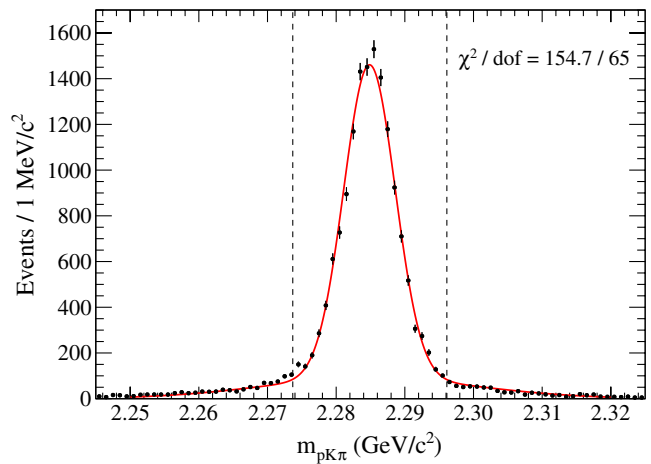


FIG. 1 (color online). Fitted $m_{pK\pi}$ distribution of correctly reconstructed B events in signal MC. The two dashed vertical lines enclose the $m_{pK\pi}$ signal region corresponding to $\pm 3\sigma$.

SEARCH FOR THE DECAY ...

(2284.85 ± 0.04) MeV/ c^2 , that corresponds to our reconstructed mass, is in agreement with the generated Λ_c^+ mass used in the simulation. To improve the signal-to-background ratio, we use only the signal region around the Λ_c^+ defined by $\pm 3\sigma$ of the narrow Gaussian function. For this selection, we achieve an efficiency of 89%. We validate our method by reconstructing the Λ_c^+ decay inclusively in the *BABAR* data. For comparison we only select $pK\pi$ combinations whose momentum is inside the momentum range of Λ_c^+ from correctly reconstructed $\bar{B}^0 \rightarrow \Lambda_c^+ \bar{p} p \bar{p}$ decays in the signal MC sample. We find that the widths and fractions of the fitted distribution to $m_{pK\pi}$ from Λ_c^+ decays in the data sample and the signal MC sample are in agreement but the mean value is shifted by 0.5 MeV/ c^2 . Thus, the signal region in the $m_{pK\pi}$ distribution in data is shifted correspondingly.

The separation of signal from background in the B candidate sample is obtained using the invariant mass m_B and the energy-substituted mass $m_{ES} = \sqrt{(s/2 + \mathbf{p}_i \cdot \mathbf{p}_B \cdot c^2)/E_i^2 - (|\mathbf{p}_B| \cdot c)^2/c^2}$, where \sqrt{s} is the CM energy of the e^+e^- pair. (E_i, \mathbf{p}_i) is the four-momentum vector of the e^+e^- CM system and \mathbf{p}_B the B -candidate momentum vector, both measured in the laboratory frame. For correctly reconstructed B decays, m_B and m_{ES} are centered at the B meson mass. Figure 2(a) shows the m_{ES} vs m_B distribution for all reconstructed B candidates, including the selection criteria for $m_{pK\pi}$. Both m_{ES} and m_B peak at the nominal \bar{B}^0 meson mass and have a correlation coefficient of 2.6%.

We define a signal region for \bar{B}^0 decay candidates in the m_{ES} - m_B plane that lies within a 3σ covariance ellipse around the nominal \bar{B}^0 mass [Fig. 2(a)]. Beside the correlation coefficient, the ellipse is defined by the mean value (μ) and the standard deviation (σ) of both variables, whose determination is described in the following section. The prefix “ 3σ ” refers to the fact that the length of the two half-axes of the ellipse is three times the σ value of m_{ES} and m_B , respectively.

We fit a single Gaussian function to the m_{ES} invariant-mass distribution yielding a mean of $\mu(m_{ES}) = (5279.44 \pm 0.03)$ MeV/ c^2 and a standard deviation of $\sigma(m_{ES}) = (2.62 \pm 0.02)$ MeV/ c^2 . As in the $m_{pK\pi}$ case, the m_B invariant-mass distribution has both a narrow and broad component and we fit it to a sum of two Gaussian functions with a common mean. We obtain a mean of $\mu(m_B) = (5279.34 \pm 0.05)$ MeV/ c^2 consistent with the nominal \bar{B}^0 mass. The narrow component contains 80% of the signal and has a standard deviation of $\sigma(m_B) = (5.26 \pm 0.07)$ MeV/ c^2 while that of the broad component is $\sigma(m_B) = (14.5 \pm 0.5)$ MeV/ c^2 . The uncertainties again are purely statistical. The selection in m_{ES} and m_B , using the described signal region, has an efficiency of 82%.

To validate the viability of our selection in the m_{ES} - m_B plane, we perform studies in the control channels $B \rightarrow \bar{D}^{(*)} D^{(*)} K$ [24] and $\bar{B}^0 \rightarrow \Lambda_c^+ \bar{p} \pi^+ \pi^-$ [5]. For both decay

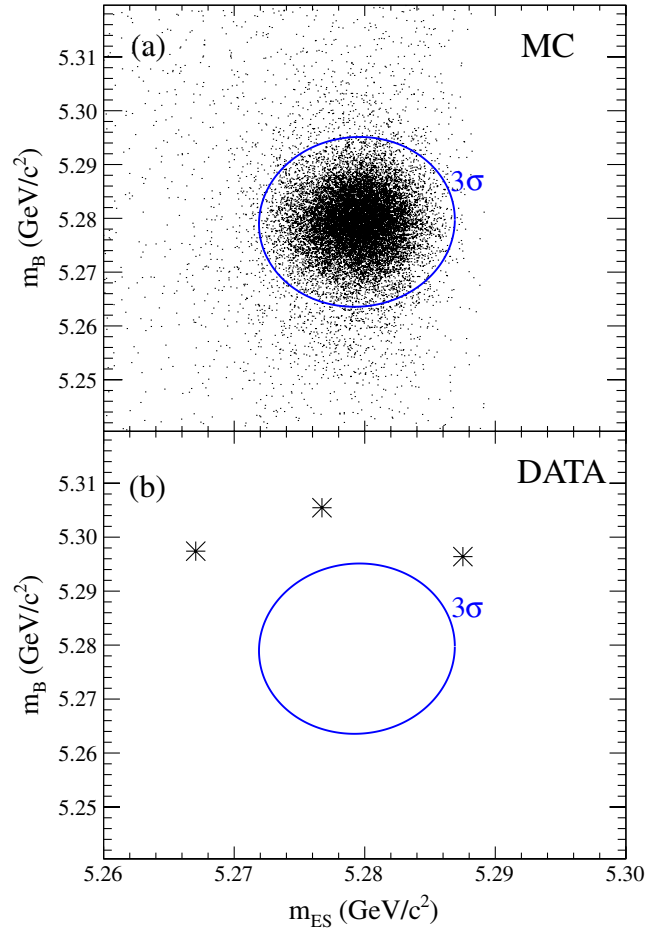
PHYSICAL REVIEW D **89**, 071102(R) (2014)

FIG. 2 (color online). The m_{ES} vs m_B distribution of selected events in (a) signal MC and (b) data. No signal candidates are observed within the signal region of the data sample.

channels, we find that the distributions of m_{ES} vs m_B in the signal MC and in the data are in agreement, confirming that our MC is able to describe the data correctly.

Figure 2(b) shows the distribution of m_{ES} vs m_B for $\bar{B}^0 \rightarrow \Lambda_c^+ \bar{p} p \bar{p}$ candidates in the data sample. Only three events remain after the selection in the vicinity of the signal region, and we do not observe any events inside the signal region.

We determine the selection efficiency from the number of reconstructed events in the signal MC sample inside the signal region normalized to the total number of generated events; this yields an efficiency of $\epsilon = (3.52 \pm 0.05)\%$. We estimate the systematic uncertainty on the efficiency by repeating the analysis in the m_{ES} vs ΔE plane, where $\Delta E = E_B^* - \sqrt{s}/2$ is the deviation from the nominal energy of the B candidate in the e^+e^- CM system. As before, we define a 3σ signal region, where we find no B candidates in the data sample, and determine the selection efficiency in the signal MC sample. The absolute difference in efficiencies is 0.02%. In addition, we account for the statistical uncertainty in the efficiency of 0.03% resulting from the limited

size of the signal MC sample. Furthermore, we estimate the uncertainty in the efficiency from tracking to be 0.03%. Summing these values in quadrature, we determine a total uncertainty of 0.05%. Other systematic uncertainties that influence the measurement of the branching fraction are due to uncertainties on the number of B events and particle identification efficiency. We find these values to be negligible compared to the uncertainty of the reconstruction efficiency in the signal MC sample.

In Eq. (2), we define a modified branching fraction (\mathcal{B}_{mod}),

$$\begin{aligned}\mathcal{B}_{\text{mod}} &= \mathcal{B}(\bar{B}^0 \rightarrow \Lambda_c^+ \bar{p} p \bar{p}) \times \frac{\mathcal{B}(\Lambda_c^+ \rightarrow p K^- \pi^+)}{0.050}, \\ &= \frac{N_{\text{observed}}}{\varepsilon \cdot N_B \cdot 0.050},\end{aligned}\quad (2)$$

which is the usual product branching fraction normalized to the world average value of $\mathcal{B}(\Lambda_c^+ \rightarrow p K^- \pi^+) = (0.050 \pm 0.013)$ [1]. N_{observed} is the number of signal events and $N_B = 471 \times 10^6$ is the number of \bar{B}^0 mesons in the *BABAR* data set, assuming equal production of $B^0 \bar{B}^0$ and $B^+ B^-$ by $\Upsilon(4S)$ decays. The definition is equivalent to $\mathcal{B}(\bar{B}^0 \rightarrow \Lambda_c^+ \bar{p} p \bar{p})$ but independent of the large external uncertainty on the branching fraction for $\Lambda_c^+ \rightarrow p K^- \pi^+$.

In a Bayesian approach, we evaluate the probability density function (pdf) of \mathcal{B}_{mod} given by N_{observed} and ε by performing pseudoexperiments and determine an upper limit at 90% C.L. We vary the value of N_{observed} and ε according to the following distributions:

$$P(x = N_{\text{observed}}) = \left[\frac{x^n}{n!} \cdot e^{-x} \right]_{n=0} = e^{-x}, \quad (3)$$

$$P(\varepsilon) = \frac{1}{\sqrt{2\pi}\sigma(\varepsilon)} \cdot \exp \left[-\frac{1}{2} \left(\frac{\varepsilon - \mu(\varepsilon)}{\sigma(\varepsilon)} \right)^2 \right]. \quad (4)$$

Equation (3) is a Poisson distribution that describes the pdf for finding no signal events ($n = 0$) given by the true number of $\bar{B}^0 \rightarrow \Lambda_c^+ \bar{p} p \bar{p}$ decays (x). Equation (4) represents a Gaussian distribution that models the pdf of the reconstruction efficiency. We use the determined efficiency as the mean value (μ) and the uncertainty on the efficiency as the standard deviation (σ). Figure 3 shows the distribution of \mathcal{B}_{mod} for the given uncertainty of $\sigma(\varepsilon) = 0.05\%$ and for a 20 times higher uncertainty of $\sigma(\varepsilon) = 1.0\%$ to assess the impact of systematic uncertainties on this quantity. We determine branching fraction upper limits at the 90% confidence level of $\text{BF} < 2.8 \times 10^{-6}$ for $\sigma(\varepsilon) = 0.05\%$ and $\text{BF} < 3.1 \times 10^{-6}$ for $\sigma(\varepsilon) = 1.0\%$, respectively. The upper limit rises to 2.9×10^{-6} only at $\sigma(\varepsilon) = 0.55\%$. This demonstrates that our result is robust against systematic uncertainties.

To summarize, we have searched for the decay $\bar{B}^0 \rightarrow \Lambda_c^+ \bar{p} p \bar{p}$ using a sample corresponding to an integrated

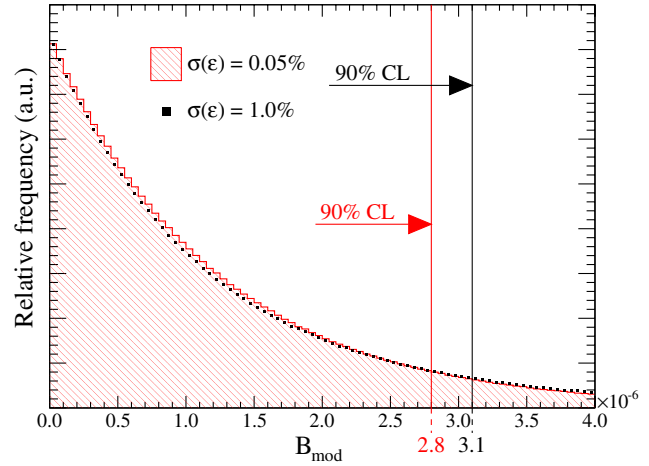


FIG. 3 (color online). The distribution of the modified branching fraction \mathcal{B}_{mod} from pseudoexperiments using the calculated uncertainty of the reconstruction efficiency $\sigma(\varepsilon) = 0.05\%$ (hatched) and a 20 times higher uncertainty $\sigma(\varepsilon) = 1.0\%$ (squares). The two vertical lines indicate the upper limit of the 90% C.L., respectively.

luminosity of 424 fb^{-1} in e^+e^- collisions at the $\Upsilon(4S)$ resonance, collected with the *BABAR* detector. We find no events and derive the upper limit on the branching fraction,

$$\begin{aligned}\mathcal{B}(\bar{B}^0 \rightarrow \Lambda_c^+ \bar{p} p \bar{p}) \times \frac{\mathcal{B}(\Lambda_c^+ \rightarrow p K^- \pi^+)}{0.050} \\ < 2.8 \times 10^{-6} \text{ at } 90\% \text{ C.L.},\end{aligned}\quad (5)$$

where we normalize the product branching fraction to the world average value of $\mathcal{B}(\Lambda_c^+ \rightarrow p K^- \pi^+) = 0.050$. We interpret the upper limit on $\mathcal{B}(\bar{B}^0 \rightarrow \Lambda_c^+ \bar{p} p \bar{p})$ in comparison to the nonresonant branching fraction of $\mathcal{B}(\bar{B}^0 \rightarrow \Lambda_c^+ \bar{p} \pi^+ \pi^-)$. We use the result $\mathcal{B}(\bar{B}^0 \rightarrow \Lambda_c^+ \bar{p} \pi^+ \pi^-)_{\text{non-}\Sigma_c} = (7.9 \pm 2.1) \times 10^{-4} = (0.64 \pm 0.17) \cdot \mathcal{B}(\bar{B}^0 \rightarrow \Lambda_c^+ \bar{p} \pi^+ \pi^-)$ published in [5]. In addition, we take into account contributions from additional intermediate states including $\bar{\Delta}^{--}$ and ρ resonances that are not accounted for in the analysis, but that are visible in the invariant mass spectra of $\bar{p} \pi^-$ and $\pi^+ \pi^-$. In summary, we estimate that $\mathcal{B}(\bar{B}^0 \rightarrow \Lambda_c^+ \bar{p} \pi^+ \pi^-)_{\text{non-res}} \approx 0.5 \cdot \mathcal{B}(\bar{B}^0 \rightarrow \Lambda_c^+ \bar{p} \pi^+ \pi^-)$. Therefore, we calculate

$$\frac{\mathcal{B}(\bar{B}^0 \rightarrow \Lambda_c^+ \bar{p} p \bar{p})}{\mathcal{B}(\bar{B}^0 \rightarrow \Lambda_c^+ \bar{p} \pi^+ \pi^-)_{\text{non-res}}} \lesssim \frac{1}{220}. \quad (6)$$

If we separate the dynamic and kinematic factors that contribute to the branching fraction according to $\mathcal{B} \sim \int |M|^2 \cdot d\text{PS} = \langle |M|^2 \rangle \times \int d\text{PS}$, where $\langle |M|^2 \rangle = \frac{\int |M|^2 d\text{PS}}{\int d\text{PS}}$ is the average quadratic matrix element of the decay, we can write

$$\frac{\mathcal{B}(\bar{B}^0 \rightarrow \Lambda_c^+ \bar{p} p \bar{p})}{\mathcal{B}(\bar{B}^0 \rightarrow \Lambda_c^+ \bar{p} \pi^+ \pi^-)_{\text{non-res}}} = r \times \frac{1}{1500}. \quad (7)$$

In Eq. (7) we applied $\frac{\int d\text{PS}(\bar{B}^0 \rightarrow \Lambda_c^+ \bar{p} p \bar{p})}{\int d\text{PS}(\bar{B}^0 \rightarrow \Lambda_c^+ \bar{p} \pi^+ \pi^-)} = \frac{1}{1500}$ and introduced an effective scaling factor r that quantifies the enhanced production rate of baryons due to dynamic effects. Using the result from Eq. (6), we obtain

$$r = \frac{\langle |M(\bar{B}^0 \rightarrow \Lambda_c^+ \bar{p} p \bar{p})|^2 \rangle}{\langle |M(\bar{B}^0 \rightarrow \Lambda_c^+ \bar{p} \pi^+ \pi^-)|^2 \rangle} \lesssim 6.8.$$

This is in tension with the quantities $\mathcal{B}(B^- \rightarrow \Lambda_c^+ \bar{\Lambda}_c^- K^-)/\mathcal{B}(B^- \rightarrow \Lambda_c^+ \bar{p} \pi^-) \approx 3$ and $\int d\text{PS}(B^- \rightarrow \Lambda_c^+ \bar{\Lambda}_c^- K^-)/\int d\text{PS}(B^- \rightarrow \Lambda_c^+ \bar{p} \pi^-) \approx \frac{1}{70}$, which leads to a factor of $r = 210$ without subtracting contributions from intermediate states in $B^- \rightarrow \Lambda_c^+ \bar{p} \pi^-$. Under the used assumptions, we conclude that a significantly enhanced decay rate of $\bar{B}^0 \rightarrow \Lambda_c^+ \bar{p} p \bar{p}$ w.r.t. $(\bar{B}^0 \rightarrow \Lambda_c^+ \bar{p} \pi^+ \pi^-)_{\text{non-res}}$ due to dynamic effects that are related to the threshold enhancement does not exist.

We are grateful for the extraordinary contributions of our PEP-II2 colleagues in achieving the excellent luminosity and machine conditions that have made this work possible. The success of this project also relies critically on the expertise and dedication of the computing organizations that support BABAR. The collaborating institutions wish to thank SLAC for its support and the kind hospitality extended to them. This work is supported by the U.S. Department of Energy and National Science Foundation, the Natural Sciences and Engineering Research Council (Canada), the Commissariat à l'Energie Atomique and Institut National de Physique Nucléaire et de Physique des Particules (France), the Bundesministerium für Bildung und Forschung and Deutsche Forschungsgemeinschaft (Germany), the Istituto Nazionale di Fisica Nucleare (Italy), the Foundation for Fundamental Research on Matter (Netherlands), the Research Council of Norway, the Ministry of Education and Science of the Russian Federation, Ministerio de Ciencia e Innovación (Spain), and the Science and Technology Facilities Council (United Kingdom). Individuals have received support from the Marie-Curie IEF program (European Union) and the A. P. Sloan Foundation (USA).

-
- [1] J. Beringer *et al.* (Particle Data Group Collaboration), *Phys. Rev. D* **86**, 010001 (2012).
 - [2] The use of charge conjugate decays is implied throughout this paper.
 - [3] J. P. Lees *et al.* (BABAR Collaboration), *Nucl. Instrum. Methods Phys. Res., Sect. A* **726**, 203 (2013).
 - [4] S. A. Dytman *et al.* (CLEO Collaboration), *Phys. Rev. D* **66**, 091101 (2002).
 - [5] J. P. Lees *et al.* (BABAR Collaboration), *Phys. Rev. D* **87**, 092004 (2013).
 - [6] P. del Amo Sanchez *et al.* (BABAR Collaboration), *Phys. Rev. D* **85**, 092017 (2012).
 - [7] B. Aubert *et al.* (BABAR Collaboration), *Phys. Rev. D* **82**, 031102 (2010).
 - [8] B. Aubert *et al.* (BABAR Collaboration), *Phys. Rev. D* **78**, 112003 (2008).
 - [9] M. Z. Wang *et al.* (Belle Collaboration), *Phys. Rev. Lett.* **92**, 131801 (2004).
 - [10] J. Z. Bai *et al.* (BES Collaboration), *Phys. Rev. Lett.* **91**, 022001 (2003).
 - [11] J. L. Rosner, *Phys. Rev. D* **68**, 014004 (2003).
 - [12] M. Suzuki, *J. Phys. G* **34**, 283 (2007).
 - [13] A. Datta and P. J. O'Donnell, *Phys. Lett. B* **567**, 273 (2003).
 - [14] G.-J. Ding and M.-L. Yan, *Eur. Phys. J. A* **28**, 351 (2006).
 - [15] A. Sibirtsev, J. Haidenbauer, S. Krewald, U.-G. Meissner, and A. W. Thomas, *Phys. Rev. D* **71**, 054010 (2005).
 - [16] B. S. Zou and H. C. Chiang, *Phys. Rev. D* **69**, 034004 (2004).
 - [17] D. J. Lange, *Nucl. Instrum. Methods Phys. Res., Sect. A* **462**, 152 (2001).
 - [18] T. Sjöstrand, *Comput. Phys. Commun.* **82**, 74 (1994).
 - [19] S. Agostinelli *et al.* (GEANT4 Collaboration), *Nucl. Instrum. Methods Phys. Res., Sect. A* **506**, 250 (2003).
 - [20] B. Aubert *et al.* (BABAR Collaboration), *Phys. Rev. D* **66**, 032003 (2002).
 - [21] B. Aubert *et al.* (BABAR Collaboration), *Nucl. Instrum. Methods Phys. Res., Sect. A* **479**, 1 (2002).
 - [22] B. Aubert *et al.* (BABAR Collaboration), *Nucl. Instrum. Methods Phys. Res., Sect. A* **729**, 615 (2013).
 - [23] T. Allmendinger, B. Bhuyan, D. N. Brown, H. Choi, S. Christ, R. Covarelli, M. Davier, and A. G. Denig *et al.*, *Nucl. Instrum. Methods Phys. Res., Sect. A* **704**, 44 (2013).
 - [24] P. del Amo Sanchez *et al.* (BABAR Collaboration), *Phys. Rev. D* **83**, 032004 (2011).